THEORETICAL AND EXPERIMENTAL DETERMINATION OF FLIGHT PERFORMANCES OF AN AIRPLANE IN MARTIAN ATMOSPHERIC FLIGHT

P. Teofilatto

Scuola di Ingegneria Aerospaziale
v. Eudossiana 18, 00184 Roma , Italy

ABSTRACT

Several missions devoted to the study of the Mars surface and enviroment have been recently proposed by NASA and ESA.
For such scientific missions, the use of a composed system having as last component an aircraft, able to fly on the Martian atmosphere, is here proposed .
Of course, realistic data on flight performances of such an aircraft can only be achieved by experimental tests.
We show that experimental results can be obtained by tests of a 0.4 scaled model flying at 25 Km of altitude from the Earth surface.
Such a scaled model has been realized at Aerospace Department of the University of Rome "La Sapienza", and its characteristic are described.
Some aerodynamical properties have been determined by approximate analytical formulas getting a first idea of the aircraft flight performances, in view of the experimental results.

INTRODUCTION

Several missions to Mars over the remainder of the decade have been decided by NASA and European partners in order to study the planet surface and enviroment, also in view of the future manned mission to Mars, planned early in the next century.
These missions require rather low planetary orbits and severe control strategies in order to keep a spacecraft on low orbits in a not completely known enviroment (see for instance the problem of life-time prediction of lunar orbiters). Moreover, lower speed flights would be more convenient for these kind of missions.
Therefore , taking advantage of the Martian atmosphere, the use of an autonomuos slow speed aircraft seems rather attractive.
The Martian enviroment is characterized by rather low gravitational field and atmospheric density. Some data about the planet are summarized in Table 1. Gravity at Mars surface is about one third of the Earth's one.
In Table 2 the components of the Standard Martian Atmosphere are reported. The atmospheric density at the Mars surface is about $\frac{1}{100}$ of the Earth density.
The variation of the Mars atmospheric density with altitude is computed according to [1] , and it is shown in Figure 1.
In the present paper an airplane suitable to a Martian flight is presented. Its design is shown and some of its aereodinamical properties are predicted analytically.
Of course it is crucial to identify experimentally its flight performances and stability derivatives.
In general, for Earth atmospheric vehicles, this is done by tests of hinged models in wind tunnels and eventually by flights of full-scale models.
However, some flight performances can be deduced from tests flights of a scaled model, which is ,of course, more convenient for economical, readiness and security reasons.
For a Martian atmospheric vehicle, the possibility to perform tests by a scaled model flying on the Earth it is even more appealing.
Namely, we shall show that the flight dynamics of a full scale airplane flying 1 Km hight above the Martian surface is equivalent to a 0.4 scaled model flying at 25 Km of altitude from the Earth.
Taking this equivalence into account, the design of a Martian airplane can be close to the existing projects of experimental Earth airplanes having the following characteristics: i) high altitude flight , ii) low velocity, iii) autonomous navigation.
NASA proposed an airplane for stratospheric flight to study Earth pollution at hight altitudes: this airplane, called Mini Sniffer, seems to satisfy the above three requirements.
Some years ago Prof. M. Sirinian of the School of Aerospace Engineering of the University of Rome "La Sapienza", designed and manifactured a prototipe, pictured in Fig 2, similar in shape (but not in the aerodynamics) to the NASA Mini Sniffer.
We think to use this prototipe as a 0.4 scaled model of the airplane intended to flight to Mars. Its properties will be reported in the next Sections: here the mission

design will be briefly described.
The mission consists of several steps: first a satellite is launched to reach a circular orbit at 50 Km of altitude from the Martian surface.
Second, a descending capsule is delivered containing the airplane with undeploied wings and tail. The velocity during the descent is reduced by a parachute. At 5 Km of altitude the lower shell of the capsule is separated from the upper one (see Fig 3).
The lower shell and the airplane will descend together (at higher velocity than the upper shell which is under the braking influence of the parachute) for the short time needed to deploy the aircraft aerodynamical surfaces and to start its hydrazine engine (Akkermann type).
Third, the airplane will leave the lower shell of the descending capsule to reach the height of 1 Km where the scientific mission begin.
The crucial phase of the airplane separation from the descent capsule as well as the aircraft flight can be simulated experimentally. Namely the 0.4 scaled model can be used as a payload of a scientific ballon and released from it at 30 Km of altitude from the Earth surface. At such height realistic separation tests as well as determination of several flight performances can be performed.
The flight data during the tests will be registred on board and navigation will be radar tracked on ground.
In the following Section the possibility to test a Martian airplane by flight tests on a scaled model at 25 Km from the Earth surface is shown.
In the last Section the characteristics of the scaled and full model are reported. Some aerodynamical properties are determined by approximated computations in order to get a first idea of the flight performances, before the tests.

Dynamical and Aerodynamical Equivalences

It is useful to predict the flight performances of a Martian atmospheric vehicle by Earth flight tests of a scaled model: it is shown here that the flight of a Martian airplane at 1 Km of altitude is equivalent to the flight of a 0.4 scaled model at 25 Km of altitude from the Earth surface.
By equivalent flights we mean that there exists a geometric similitude between the trajectories. This is achieved if there are linear relations between the position vectors and the reference times.
That is , denoting by subscript 1 the terms relative to the model and by subscript 2 the terms of the full scale vehicle, we have:

$$\vec{x}_1(t_1) = k\,\vec{x}_2(t_2) \quad , \quad t_1 = \tau\, t_2 \tag{1}$$

where k and τ are constants (to be determined).
The model and the real airplane have the same geometry, and if l_1, l_2 are characteristic lenghts of the model and of the real airplane respectively, there is the geometrical similarity condition:

$$l_1 = \lambda\, l_2$$

with scale factor λ.
As a consequence of relation (1), we get the following relations between the velocity and the acceleration vectors:

$$\begin{cases} \vec{v}_1 = \dfrac{d\vec{x}_1}{dt_1} = k\dfrac{d\vec{x}_2}{dt_2}\dfrac{dt_2}{dt_1} = \dfrac{k}{\tau}\vec{v}_2 \\ \vec{a}_1 = \dfrac{d\vec{v}_1}{dt_1} = \dfrac{k}{\tau}\dfrac{d\vec{v}_2}{dt_2}\dfrac{dt_2}{dt_1} = \dfrac{k}{\tau^2}\vec{a}_2 \end{cases} \tag{2}$$

Both the vehicles are subjected to gravity and aeropropulsive forces $\vec{G}_i$, $\vec{A}_i$, $i = 1, 2$. Since position and velocity are just scaled, we can consider relations on the moduli of the forces only: these are required to be in constant ratio:

$$\frac{G_1}{G_2} = \frac{m_1 g_1}{m_2 g_2} = \frac{A_1}{A_2} = h \tag{3}$$

As a consequence of (3) we get also:

$$\frac{m_1 a_1}{m_2 a_2} = h \tag{4}$$

By (3) and (4) it follows:

$$\frac{k}{\tau^2} = \frac{a_1}{a_2} = \frac{g_1}{g_2}$$

Since the gravitational constant of the Earth g_1 is almost 3 times the gravitational constant of Mars g_2, we get:

$$\tau = \sqrt{\frac{k}{3}}$$

Again from relations (3) and (4) we get:

$$\frac{m_1 a_1}{m_2 a_2} = \frac{m_1}{m_2}\frac{k}{\tau^2} = \frac{A_1}{A_2} = \frac{\frac{1}{2}\rho_1 v_1^2 S_1 C_1}{\frac{1}{2}\rho_2 v_2^2 S_2 C_2}$$

where C_1 and C_2 are the aerodynamic coefficients: these must be equal according to the aerodynamical equivalence (see later), then the two masses are related by:

$$\frac{m_1}{m_2} = \frac{\tau^2}{k}\frac{\rho_1}{\rho_2}\left(\frac{k}{\tau}\right)^2\lambda^2 = k\lambda^2\frac{\rho_1}{\rho_2} \tag{5}$$

Relations (1) and (2) refer to the motion of the center of mass: the attitude motion of the two vehicles will follow the Euler equations:

$$\underline{I}_1\,\dot{\underline{\omega}}_1 + \underline{\omega}_1 \wedge \underline{I}_1\,\underline{\omega}_1 = \underline{M}_1 \tag{6}$$

$$\underline{I}_2\,\dot{\underline{\omega}}_2 + \underline{\omega}_2 \wedge \underline{I}_2\,\underline{\omega}_2 = \underline{M}_2 \qquad (7)$$

We require linear relations:

$$\underline{M}_1 = s\,\underline{M}_2 \qquad (8)$$

$$\underline{\omega}_1 = r\,\underline{\omega}_2 \qquad (9)$$

In particular from (8) :

$$s = \frac{M_1}{M_2} = \frac{\frac{1}{2}\rho_1 v_1^2 S_1 l_1 C_m(1)}{\frac{1}{2}\rho_2 v_2^2 S_2 l_2 C_m(2)} = \frac{\rho_1}{\rho_2}\frac{k^2}{\tau^2}\lambda^3$$

and from (9) :

$$\dot{\underline{\omega}}_1 = \frac{r}{\tau}\dot{\underline{\omega}}_2$$

The relation between the two inertia diadics is :

$$\underline{I}_1 = \frac{\rho_1}{\rho_2}\lambda^4 k\,\underline{I}_2 \qquad (10)$$

Formula (10) can be proved recalling the definition of the inertia diadic:

$$\underline{I}_1 = \sum_{i=1}^{N} m_i(1)[r_i^2(1)\underline{u} - \vec{r}_i(1)\,\vec{r}_i(1)]$$

(where sum rather than integration is used for convenience).

Since $r_i(1) = \lambda r_i(2)$ and (by relation (7)) $m_i(1) = k\lambda^2\frac{\rho_1}{\rho_2}m_i(2)$, we get relation (10). It follows that equation (6) can be written as:

$$\frac{\rho_1}{\rho_2}\lambda^4 k\frac{r}{\tau}\underline{I}_2\dot{\underline{\omega}}_2 + r^2\frac{\rho_1}{\rho_2}\lambda^4 k\,\underline{\omega}_2 \wedge \underline{I}_2\underline{\omega}_2 = \frac{\rho_1}{\rho_2}\frac{k^2}{\tau^2}\lambda^3\underline{M}_2$$

The above equation holds true, according to (7), if $r = \frac{1}{\tau}$ and $k = \lambda$.

Therefore the dynamical equivalences

$$\vec{x}_1 = \lambda\vec{x}_2$$

$$\vec{v}_1 = \sqrt{\frac{g_1}{g_2}}\lambda\vec{v}_2 \sim \sqrt{3\lambda}\vec{v}_2$$

$$\underline{\omega}_1 = \sqrt{\frac{g1/g2}{\lambda}}\underline{\omega}_2 \sim \sqrt{\frac{3}{\lambda}}\underline{\omega}_2$$

are satisfied once the aerodynamical equivalences $C_1 = C_2$, $C_m(1) = C_m(2)$ are given.

As known (see for instance [2, p.77]), the aerodynamical equivalence for similar bodies in incompressible flow is ensured if their related Reynolds numbers are equal. If compressibility has to taken into account, the Mach numbers numbers have to be equal also. However since the Mach range of both the vehicles is rather low, only Reynolds equivalence will be imposed.

Then, if ν_1, ν_2 denote the kinetic viscosities, it is necessary to have:

$$Re_1 = \frac{V_1\,l_1}{\nu_1} = Re_2 = \frac{V_2\,l_2}{\nu_2}$$

hence

$$1 = \frac{V_1}{V_2}\frac{l_1}{l_2}\frac{\nu_2}{\nu_1} = \frac{k}{\tau}\lambda\frac{\nu_2}{\nu_1} = \sqrt{3}\lambda^{\frac{3}{2}}\frac{\nu_2}{\nu_1}$$

that is

$$\lambda = 0.69(\frac{\nu_1}{\nu_2})^{\frac{2}{3}}$$

At 1 Km of altitude the kinetic viscosity of the Martian atmosphere is equal to $\nu_2 = 8.5\,10^{-4}\,\frac{m^2}{sec}$; then it is possible to get a reasonable value of the scale factor , e.g. $\lambda = 0.4$, at 25 Km of altitude on the Earth atmosphere (where $\nu_1 = 3.7\,10^{-4}\,\frac{m^2}{sec}$). [1]

The Airplane Characteristics

The design and the dimensions of the airplane are in Figure 4 where dimensions in brackets refer to the 0.4 scaled model.

The general configuration of the airplane is similar to the NASA Mini Sniffer , however wing, fusolage and tail surfaces sections are rather different.

The right wing planform is in Figure 5. The section profiles are obtained by projections of the Eppler E.203 profile, as described in [3]. The wing span is equal to $b = 6.7m$ ($[2.68]m$) and the wing surface is equal to $S = 4.365m^2$ ($[0.698]m^2$), hence the aspect ratio $\frac{b^2}{S}$ is equal to 10.28. The sweep is equal to 20^o, the diedral angle is equal to -3^o and there is no twist along the span.

The elevator has a rectangular planform of dimensions $2 \times 0.375m$ ($[0.8 \times 0.15]m$): it has a constant section corresponding to the NACA $65_1 - 012$ profile.

The airplane is endowed with two rudders of trapezoidal shape with dimensions $(0.5, 0.25) \times 1.10$ meters $((0.2, 0.1) \times 0.44)$. The section is costant and it corresponds to the NACA 65-009 profile.

The fusolage shape, dimension and section are in Figure 6.

The total mass of the manifactured model is $8Kg$. Because of relation (5):

$$m_1 = \lambda^3\frac{\rho_1}{\rho_2}m_2 = (0.4)^3\frac{4 \times 10^{-2}}{1 \times 10^{-2}}\,m_2$$

the mass of the full scale airplane has to be $m_2 \sim 4m_1 = 32Kg$.

In view of the experimental tests, it is useful to have an approximate polar diagram of the airplane. Since this polar is just a starting point for the future experimental results, we avoid complex computations requiring strong numerical efforts, and relayed on the simplified model of vortex distribution along the span $b(y)$ of the

[1] Note that Martian flights at 1 Km of height would correspond to tests at Earth surface if $\lambda \sim 0.04$, probably a scale factor too much low for the technologies at our disposal at present.

aerodinamic surfaces [4]:

$$\Gamma(y) = 4\pi a(y) V_\infty (\alpha(y) + \frac{w_0}{V_\infty}) \qquad (11)$$

where $4\pi a(y) V_\infty \alpha(y)$ is the vorticity of the section of the surface at y of the two dimensional theory, and $(\alpha(y) + \frac{w_0}{V_\infty})$ is the effective angle of attack being the sum of the angle of the velocity at infinity and the down-wash angle

$$\frac{w_0}{V_\infty} = \frac{1}{V_\infty} \int_{-\frac{b}{2}}^{\frac{b}{2}} \frac{\Gamma'(\eta)}{\eta - y} d\eta$$

Instead of solving the integro-differential equation (11), the function w_0 is found as $\frac{\partial \phi}{\partial z}$ where ϕ is the potential in the two dimensional flow in the plane $x = 0$ where the slit $[-\frac{b}{2}, \frac{b}{2}]$,representing the wing leading edge , lies .

Since the vorticity distribution on the slit is $\frac{\Gamma}{2}$, the difference in potential on the upper and lower sides of the slit is :

$$\phi_- - \phi_+ = \frac{\Gamma}{2}$$

then, assuming the potential on the sides of the slit to be equal except for sign, one has $4\phi = \Gamma$ [4].

Therefore, the problem is to find an harmonic function ϕ with boundary condition on the slit:

$$4\phi = 4\pi a(y) V_\infty (\alpha(y) + \frac{1}{V_\infty} \frac{\partial \phi}{\partial z})$$

Mapping the slit to the unit circle the problem to be solved is now:

$$\begin{cases} \Delta\phi = 0 & outside\, the\, unit\, circle \\ \phi(\theta) + A\frac{\partial \phi}{\partial n} = B & on\, the\, unit\, circle \end{cases} \qquad (12)$$

where the second equation is the boundary condition on the slit transformed in the circle [see 4, p.174].

If the solution ϕ is written in an odd Fourier series

$$\phi = \frac{b}{2} V_\infty \sum_{n=1}^{\infty} \frac{B_n}{r^n} sin(n\theta)$$

the boundary condition in equation (12) becomes

$$\sum_{n=1}^{\infty} B_n sin(n\theta)(1 + \frac{\mu n}{sin\theta}) = \mu\alpha \qquad (13)$$

where $\mu = \frac{4\pi a}{2b}$.

Then vorticity and down-wash angle are

$$\Gamma(y) = 4\phi_{r=1} = 2b \sum_{n=1}^{\infty} B_n sin(n\theta)$$

$$w(y) = \frac{\partial \phi}{\partial z} = \frac{2}{b sin\theta} (\frac{\partial \phi}{\partial r})_{r=1} = -V_\infty \sum_{n=1}^{\infty} n B_n \frac{sin(n\theta)}{sin\theta}$$

and one gets the lift and drag forces:

$$L = \rho V_\infty \int_{-\frac{b}{2}}^{\frac{b}{2}} \Gamma(y) dy = \frac{\rho}{2} V_\infty^2 S^2 \pi B_1$$

$$D = -\rho \int_{-\frac{b}{2}}^{\frac{b}{2}} \Gamma(y) w(y) dy = \frac{\rho}{2} V_\infty^2 S^2 \pi B_1^2 (1 + \delta)$$

with

$$\delta = \sum_{n=2}^{\infty} \frac{n B_n^2}{B_1^2}$$

Fixing n values of θ in equation (13) it is possible to solve the resulting n equations for the first n coefficients B_n [2,pag.251].

Since the wing has not a small sweep angle, the method has to be modified according to [5]. The resulting wing polar diagram is shown in Figure 7.

This polar diagram has been tested with the one obtained by a more accurate numerical program [6], showing a good corrispondence.

The aereodynamic properties of the tail surface can be approximated by the two dimensional theory (by a second order approximation of the Theodorsen quasi-circle of the NACA profile), since the configuration of two rudders makes the tail surface like an "infinite wing".

The polar diagrams of each of the aerodynamical surface taken alone are matched by usual empirical formulas (see [3]), to get the polar of the aircraft, where also the fusolage effect is taken into account, but the mutual interference between the various surfaces has been neglected (although it could be relevant, mainly for the elevator/rudder system).

The polar diagram of the complete aircraft is shown in Figure 9 and it provides a first basis for the experimental tests.

References

1. M.D. Sirinian: "Flight on Mars" (in italian), IA.R - 20 -80, pp.1-31 (1980).
2. R.von Mises: "Theory of flight", Dover, pp.1-629 (1958).
3. M.D.Sirinian,R.Carbonaro: "Test flights of remote controlled aircrafts" (in italian), RT-DAURS 94.02 , pp.1-92 (1994).
4. R.von Mises,K.Friedrichs: "Fluid Dynamics", Applied Mathematical Sciences n. 5 , pp.1-353 (1972).
5. J. Weissinger: "The lift distribution of swept-back wings", NACA TN 1120, pp.1-38 (1942). reprinted (1983).
6. P.Gasbarri-P.Santini: "Unsteady Aerodynamics in subsonic regimes" , to be published (1996).

Period of Rotation	$24^h 37^{min} 22.7^{sec}$
Equatorial radius	3393.4 (Km)
Polar radius	3375.8 (Km)
Gravitational const.	42906 ($\frac{Km^3}{s^2}$)
Gravity at surface	3.71 ($\frac{m}{sec^2}$)
Density at surface	0.01662 ($\frac{kg}{m^3}$)
Temperature at surface	225 (K)

Table 1: Astronomical data of Mars.

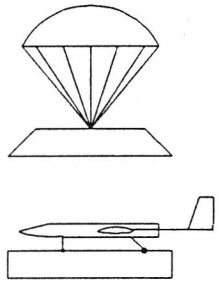

Figure 3: Scketch of the descent capsule

Constituent	p.c. in volume	mol. weight (Kg/mole)
CO_2	93.08	0.044
N_2	4.14	0.028
Ar	2.30	0.029
O_2	0.17	0.032
CO	0.11	0.028
H_2O	0.07	0.018
$Others$	0.12	0.052

Table 2: Composition of the Mars Atmosphere.

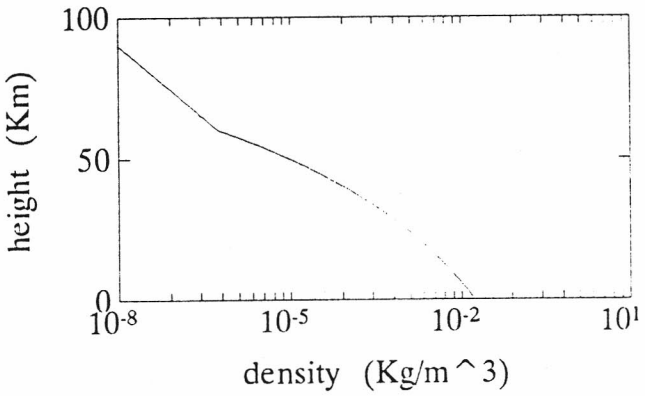

Figure 1: Mars Standard Atmosphere

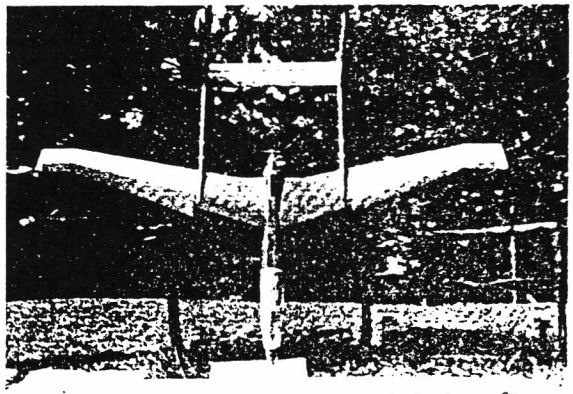

Figure 2: Picture of the 0.4 scaled aircraft

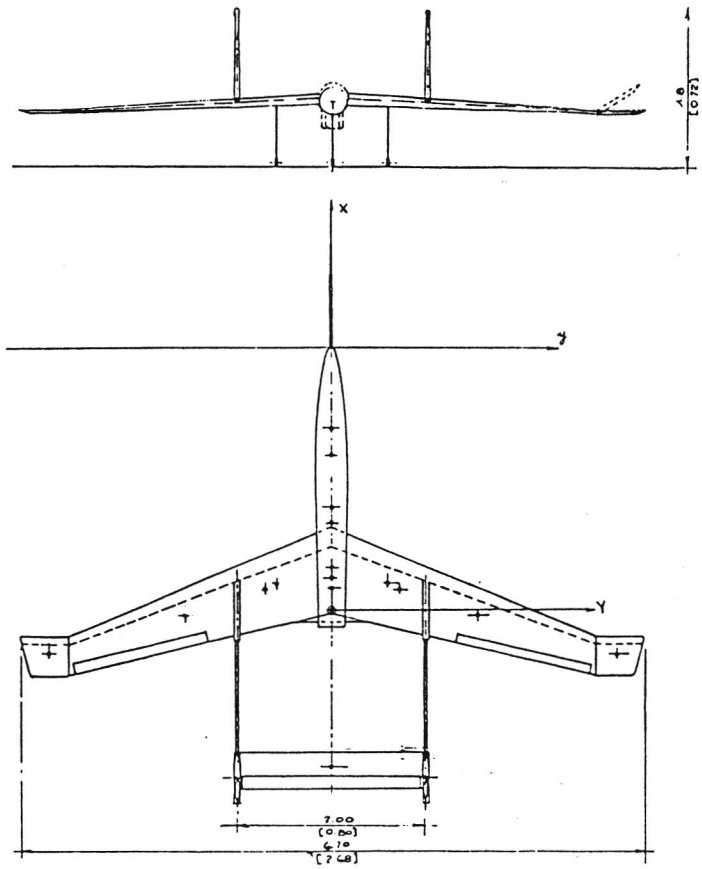

Figure 4: Airplane design (from Ref.3)

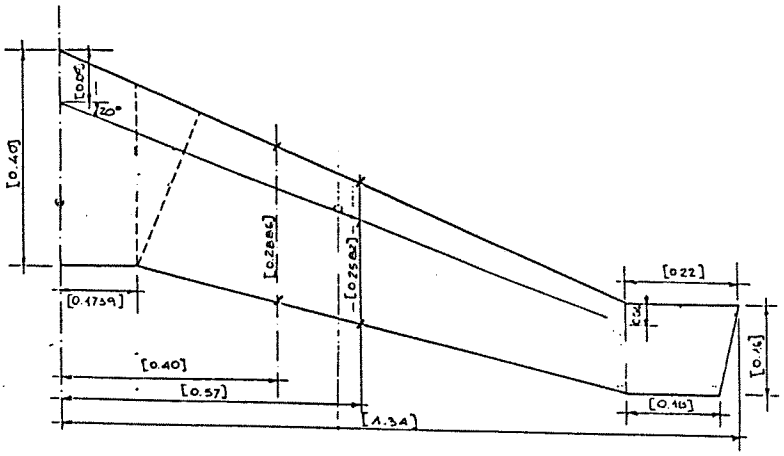

Figure 5: The right semi-wing of the model (from Ref.3)

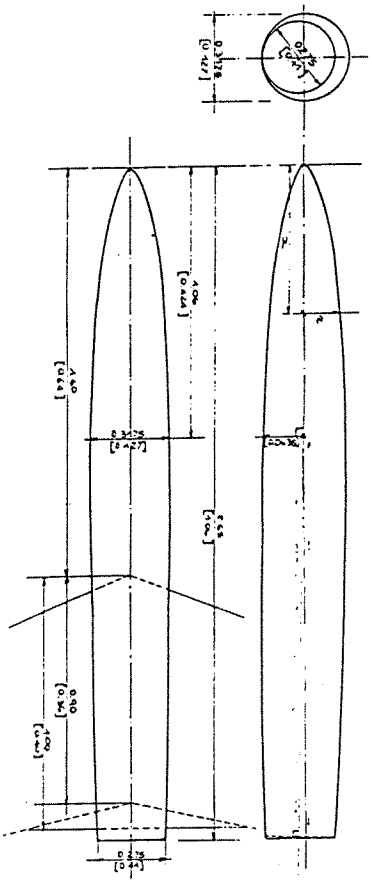

Figure 6: The fusolage (from Ref.3)

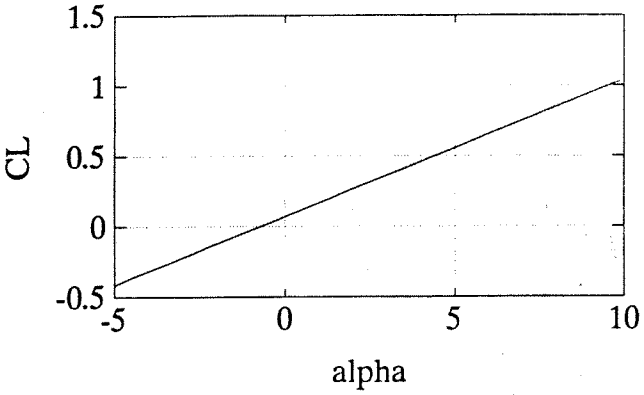

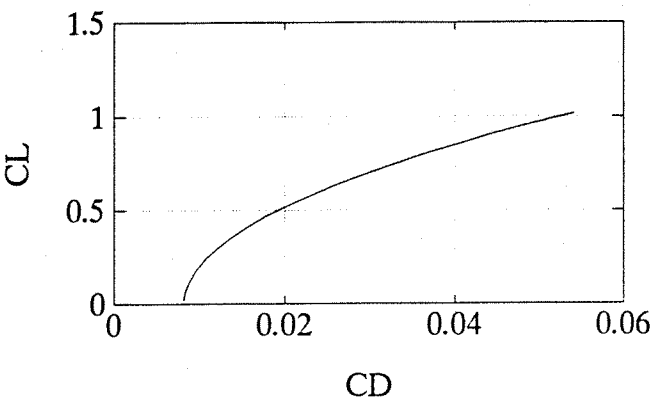

Figure 7: Wing polar diagram

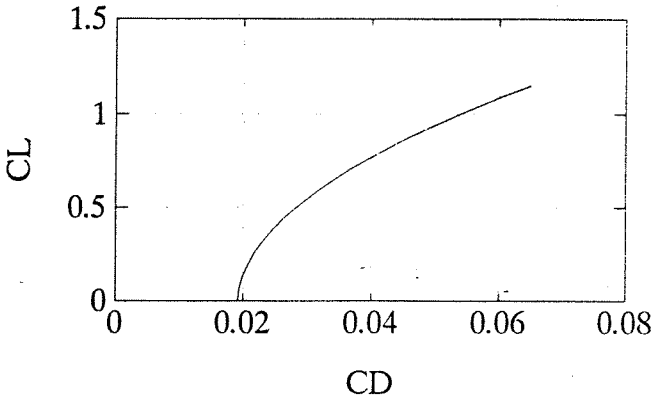

Figure 8: Airplane polar diagram